ELSEVIER

Engineering Geology 58 (2000) 337–351

ENGINEERING GEOLOGY

www.elsevier.nl/locate/enggeo

Seismically induced landslide displacements: a predictive model

Roberto Romeo *

Servizio Sismico Nazionale (SSN) Via Curtatone 3, I-00185 Rome, Italy

Received 6 November 1998; accepted for publication 16 February 2000

Abstract

Newmark's model for predicting earthquake-induced landslide displacements provides a simple way to predict the coseismic displacements affecting a sliding mass subject to earthquake loading. In this model, seismic slope stability is measured in terms of critical acceleration, which depends on the mechanical soil properties, pore-pressure distribution, and slope geometry. The triggering seismic forces are investigated in terms of energy radiation from the source, propagation, and site effects, based on 190 accelerometric recordings from 17 Italian earthquakes with magnitudes between 4.5 and 6.8. The method is based on the calibration of relations having the general form of an attenuation law that relates the energy of the seismic forces to the dynamic shear resistances of the sliding mass to propagate the expected landslide displacements as an inverse function of the distance from the fault rupture; the amount of displacement computed through these relations provides a criterion to predict the occurrence of slope failures. Finally, maps showing, in a deterministic and a probabilistic way, the potential of seismically induced landslide displacements are displayed as a tool to provide seismic landslide scenarios and earthquake-induced landslide hazard maps, respectively.

Keywords: Attenuation relations; Landslide displacement; Newmark's method; Probability maps; Seismic hazards

1. Introduction

Landslides are among the most hazardous effects of earthquakes (Keefer, 1984). This relevance has been further confirmed by the analyses of the earthquake-induced ground failures in Italy based on the historical information about landslides, surface fracturing and faulting, liquefaction, and topographic changes contained in the National Catalogue of Ground Effects Induced by Strong Earthquakes (C.E.D.I.T., release 1.1; Romeo and Delfino, 1997)[1].

The stability of slopes subject to earthquake loading can be evaluated using several methods. Currently most seismic codes, including Italian and European codes (see 'Decree of the Italian Ministry of Public Works March 11, 1988', 'Eurocode 7: Geotechnical Design', and 'Eurocode 8: Design Provisions for Earthquake Resistance of Structures'), use an ultimate-limit-state design criterion for the evaluation of the safety conditions

* Tel.: +39-06-4444-2276. fax: +39-06-4466-579.

E-mail address: roberto.romeo@dstn.it and fromeo@tiscabinet.it (R. Romeo)

[1] The catalog is available at the following Internet address: http://www.dst.it/ssn/RT/rt9704/frameset.html.

0013-7952/00/$ - see front matter
PII: S0013-7952(00)00042-9

of embankments and slopes. These can be evaluated through ordinary limit-equilibrium methods or stress analyses, expressing the stability of a slope in terms of an overall safety factor (SF) or safety margin (SM), i.e., as the ratio or the difference between available and mobilized shear strengths.

Another way to express the seismic stability of a slope is by applying Newmark's sliding block method (Newmark, 1965), which estimates the expected coseismic displacements for a given recorded or artificial acceleration time history. The method has undergone several modifications and improvements (Sarma, 1981; Wilson and Keefer, 1983), and several relations between seismic ground-motion parameters and computed landslide displacements have been proposed (Ambraseys and Menu, 1988; Jibson, 1993; Ambraseys and Srbulov, 1995).

Jibson (1993), using selected strong-motion records, computed Newmark displacements as a function of the critical acceleration needed to bring the slope to limit equilibrium (SF = 1 or SM = 0) and correlated them with the Arias intensity as the most comprehensive parameter expressing the energy content of an earthquake ground-motion record. He formulated a very simple and useful relation that allows estimation of landslide displacement if the expected Arias intensity and critical acceleration of the slope are known.

In this work, the methodology outlined by Jibson (1993) has been applied to Italian strong ground-motion records, developing new relations having the form of an attenuation equation of the expected landslide displacements as a function of earthquake magnitude and fault or epicentral distance.

These relations can be used to formulate scenarios of earthquake-induced landslide displacements, as well as to predict exceedance probabilities of fixed values of landslide displacements, as in ordinary seismic hazard assessments.

2. Seismic parameters of earthquake ground motion

The most commonly used parameter to describe earthquake ground motion is peak ground acceleration (PGA). All the analyses that follow have been carried out using a strong-motion database composed of 190 digitized accelerograms (95 couples of EW and NS horizontal components) from the recordings of 17 Italian earthquakes with magnitudes ranging from 4.6 to 6.8 (Sabetta and Pugliese, 1996). The acceleration time histories required to be baseline- and instrument-corrected with a filter in the frequency domain. The bandpass frequencies (between 0.2 and 0.5 Hz for the high-pass filtering and between 25 and 30 Hz for the low-pass filtering) were selected in order to maximize the signal-to-noise ratio. The filtering process reduced the PGA values by an average of about 3%. For each record, the epicentral distance (RE) and the closest distance to the surface projection of the fault rupture (RF) are provided. Each recording site is also classified as rock (firm soil) or alluvium (medium/soft soil), according to the local shear-wave velocity (above or below 800 m/s, respectively).

One of the most comprehensive measures of the energy content of a strong-motion recording is the Arias intensity (I_A; Arias, 1970), which dimensionally is a velocity and is given by:

$$I_A = \frac{\pi}{2g} \int_0^{t_f} [a(t)]^2 \mathrm{d}t \tag{1}$$

where g is the acceleration due to gravity, $a(t)$ is the recorded acceleration time-history and t_f is the duration of the ground motion, for which has been adopted the definition given by Vanmarke and Lai (1980), who proposed the following simplified expression for t_f:

$$t_f \cong 7.5 \frac{I_o}{a_{max}^2} \tag{2}$$

where a_{max} is the maximum recorded acceleration (PGA) and I_o is the integral over time of the squared accelerations ($I_o = I_A 2g/\pi$).

The Arias intensity is proportional to the root mean square acceleration (RMSA in cm/s^2; Housner, 1975):

$$\mathrm{RMSA} = \sqrt{\left(\frac{1}{t_f} \int_0^{t_f} [a(t)]^2 \, \mathrm{d}t\right)} \tag{3}$$

which represents the equivalent effective acceleration in the ground motion duration, t_f, that is:

$$\mathrm{RMSA} = \sqrt{\frac{I_A 2g}{\pi t_f}}. \quad (4)$$

RMSA is well correlated with PGA, giving the following linear relationship for the data set used in this study:

$$\mathrm{RMSA} = 0.14\mathrm{PGA} \quad (5)$$

where PGA and RMSA are expressed in cm/s^2, and the regression has an adjusted squared correlation coefficient of 0.81. More refined relations of I_A and RMSA as a function of PGA invoking a power law correlation are shown in Fig. 1. These allow simple estimates of I_A or, alternatively, RMSA for a given value of PGA.

3. Dynamic stability analysis

Seismic forces acting on a slope induce accelerations, whose direction and magnitude vary at any instant and from point to point in the body of the landslide.

Spatial variability of accelerations is generally overcome by engaging a resulting vector applied in the center of gravity of the landslide body. Furthermore, the temporal variability of the resulting acceleration vector determines the continuous variation of the safety factor and the available shear strengths and not simultaneously mobilized along the sliding surface. Therefore, even if a reliable dynamic safety factor could be evaluated, this provides no information about the stability conditions reached by the landslide mass after the seismic shaking.

Moreover, pseudostatic approaches, incorporating PGA for seismic stability analyses, generally underestimate the safety factor of the slope. An effective acceleration (such as RMSA) could be better assumed as representative of a pulse of constant acceleration with a rectangular shape acting for the entire strong-motion duration.

Newmark's method overcomes these problems by computing the cumulative coseismic displace-

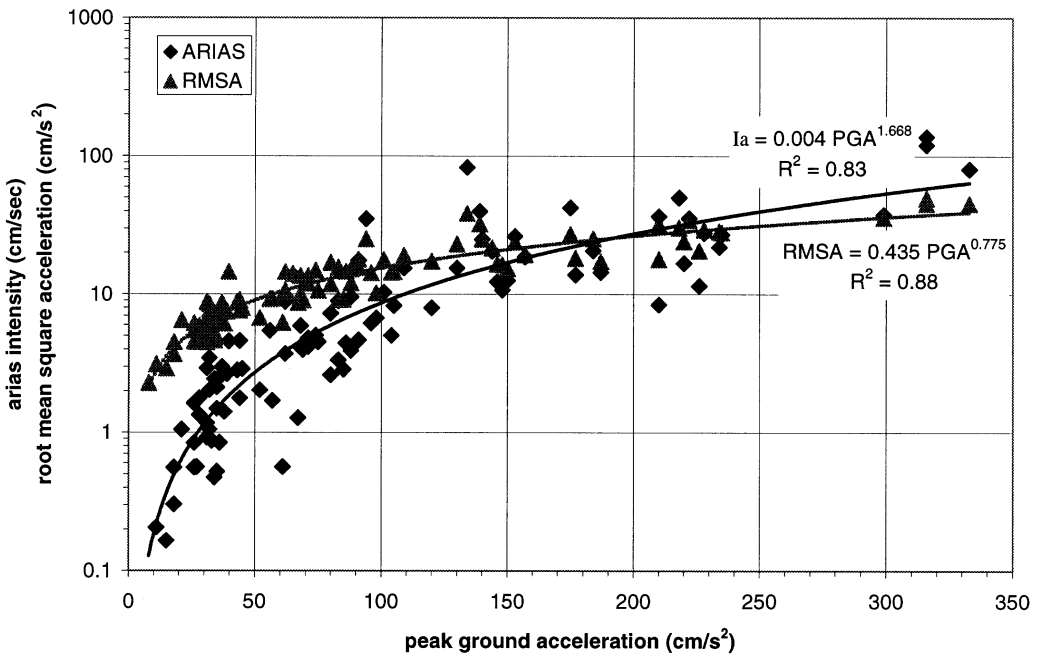

Fig. 1. Relationships among Arias intensity, root mean square acceleration and peak ground acceleration (Italian strong-motion database).

ment of the landslide mass taking into account strong-motion duration, frequency content, and stochastic variability of the seismic motion of the entire acceleration time history.

The required input to perform a Newmark analysis are a digitized acceleration time history and the critical acceleration needed to reach the limit equilibrium (SF = 1 or SM = 0).

The common assumptions and limitations involved in Newmark's method are:

1. the sliding mass is assumed to be a rigid-plastic body;
2. no permanent displacements are allowed for accelerations below the critical acceleration;
3. plastic deformations on the sliding surface are allowed when the critical acceleration is exceeded;
4. the critical acceleration is not strain-dependent;
5. static and dynamic strengths are considered to be the same and constant;
6. no pore-water pressure increment is considered.

Anyway, some of these assumptions can be removed by the analyst.

The last two assumptions can represent limitations too restrictive to perform a reliable displacements analysis. In fact, strain-softening soils can undergo large shear-strength degradation under cyclic strain; shear strengths, after reaching peak values, suddenly decrease toward residual values. Again, residual shear strengths imply lower values for the critical acceleration, increasing the cumulative displacement reached by the landslide mass after the seismic shaking. Thus, performing a Newmark analysis assuming peak shear strengths could underestimate the final coseismic displacements. On the contrary, rate effects on shear strength parameters due to fast shearing, strain-hardening materials, and soils that display a viscoplastic response due to dynamic pore-pressure effects (Jibson and Harp, 1996), can actually produce an overestimation of the coseismic displacements when Newmark's methodology is applied.

The stability conditions after the earthquake shaking can be assessed in terms of critical displacement. Critical displacement is defined as the coseismic displacement beyond which ground cracking is produced, shear strengths along the sliding surface approach residual values, and a general failure of the landslide mass may occur. The critical displacement depends on the rheological behavior of the landslide mass. Masses that display a brittle behavior (i.e., coherent and disrupted slides, and falls) have a lower critical displacement than masses whose ductility accommodates greater deformations prior to sliding (i.e., lateral spreads and flows). In this study, failures occurring in rocky slopes (disrupted falls and slides) have been assimilated to the first category, for which a critical displacement of 5 cm (Wieczorek et al., 1985) has been assumed, while a critical displacement of 10 cm has been assumed for flows and slides occurring in cohesive soils (Jibson and Keefer, 1993).

After the earthquake, for those landslides exceeding the critical displacement, a static analysis with residual shear strengths can be performed to evaluate post-seismic safety conditions (Jibson and Keefer, 1993). Two cases arise:

1. the static safety factor in residual strength conditions is less than 1, or the corresponding safety margin is less than 0: the slope is not stable and undergoes a general failure;
2. the static safety factor in residual strength conditions is greater than 1 or the corresponding safety margin is greater than 0: the slope is stable and deformation will cease after the end of the seismic shaking. However, the final displacement will range from the displacement computed with peak shear strengths (maximum value of the critical acceleration) to the displacement computed with residual shear strengths (minimum value of the critical acceleration). The latter allows the upper bound of the expected displacements to be estimated and overcomes the problem of considering critical acceleration to be strain-independent.

In saturated soils, the pore-water pressure can rise due to transient loads; in loose soils, the water pressure can balance the effective stress causing the soil to liquefy (cyclic or dynamic liquefaction). In dense soils, water pressure results in an increase of the shear strengths during the cyclic loading due to dilation; this will increase the short-term stability conditions of the slope. After the earthquake, however, the shear strengths decrease due to the generation of positive pore pressures, and

thus the long-term stability conditions of the slope become worse than the short-term stability conditions. This mechanism explains the delay of hours and even days between seismic shaking and significant landslide movements in overconsolidated clays and dense sands.

To determine the critical acceleration, conventional stability analyses to compute the static safety factor of the slope are generally performed. In Fig. 2, an infinite slope and a rotational slide are pictured to show the different significance of the slope/thrust angle, β (Newmark, 1965). The critical acceleration coefficient, K_c, acting parallel to the slope is given by the critical acceleration normalized to acceleration of gravity.

For the simplest model of an infinite slope with a steady seepage parallel to slope, the static safety factor is given by (Lambe and Whitman, 1979):

$$\mathrm{SF} = \frac{\dfrac{c'}{\gamma z}\dfrac{1}{\cos\beta} + (1-r_u)\cos\beta\tan\phi'}{\sin\beta} \quad (6)$$

where z is the depth of the sliding surface from the ground level, r_u is the pore pressure coefficient (Bishop, 1954), and c' and ϕ' are the effective shear-strength parameters. The relation overcomes the problem of performing a stability calculation in terms of total stresses. In fact, dynamic stability analyses are commonly carried out implementing the undrained shear strength of the soil, although, strictly, an effective stress analysis should be performed, taking into account the proper value of pore-water pressure developed during the cyclic loading. The proper r_u value under undrained loading can be evaluated through rigorous analyses of pore-pressure generation (Martin and Seed, 1978) or through simplified procedures (Matsui et al., 1980).

The critical acceleration coefficient is given by:

$$K_c = (\mathrm{SF}-1)\sin\beta \quad (7)$$

if K_c is acting parallel to the slope and by:

$$K_c = (\mathrm{SF}-1)\tan\beta \quad (8)$$

if K_c is acting horizontally.

Strictly speaking, critical acceleration should be defined in direction parallel to the sliding surface along which the landslide mass moves downslope. However, for practical purposes, the analysis is often simplified by taking into account horizontal acceleration and neglecting the vertical component of the ground motion, which contributes little to the instability conditions. In the following, critical acceleration is always referred to K_c, unless a different definition is explicitly given.

As an illustration of Newmark's method, Fig. 3 shows the coseismic displacement computed for the lower part of the Calitri landslide (Hutchinson and Del Prete, 1985; Crespellani et al., 1996) triggered by the Irpinia 1980, Ms 6.8 earthquake (Bernard and Zollo, 1989). When accelerations exceed the critical acceleration, the relative velocity between the block and its base increases until the acceleration drops below the threshold acceleration. The cumulative displacement continues to increase owing to inertial forces, and stops when the velocity becomes zero.

The resulting cumulative displacement is then

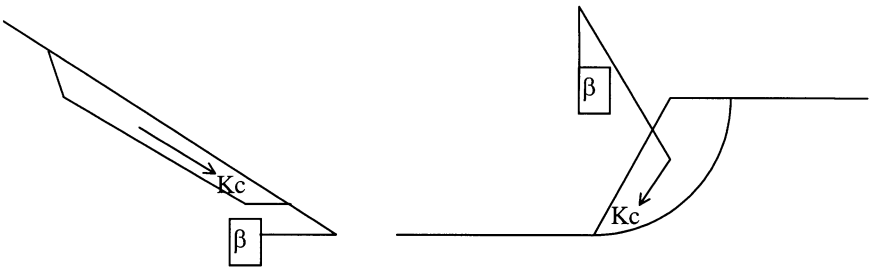

Fig. 2. Infinite slope (left) and rotational slide (right). K_c refers to tangential critical acceleration; β is the slope angle (infinite slope) or the thrust angle (rotational slide).

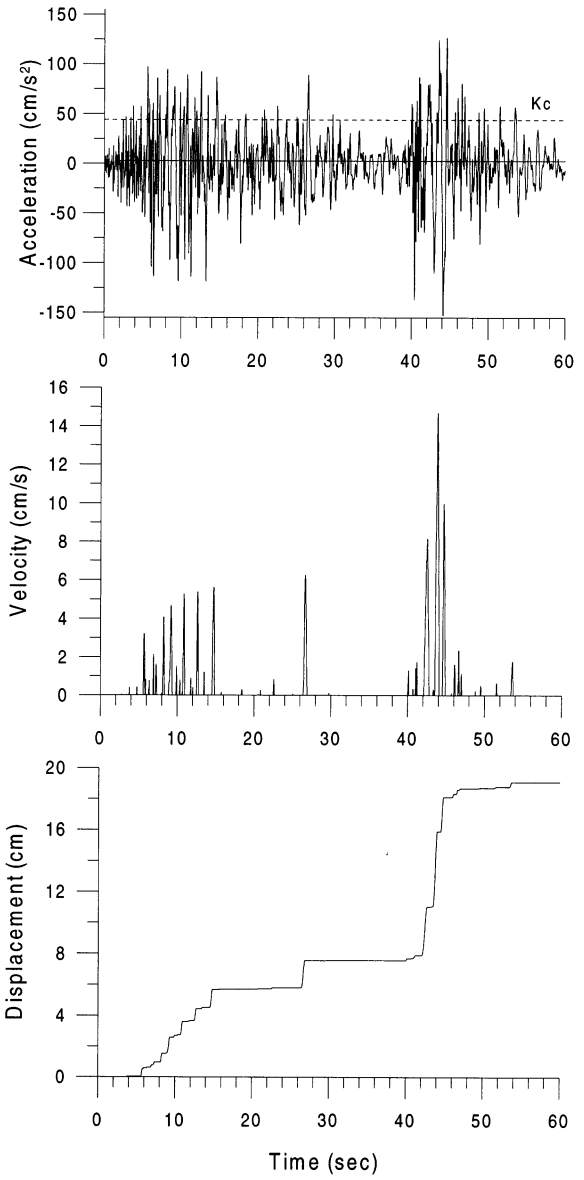

Fig. 3. Newmark's approach to coseismic landslide displacement computation. Example from the Calitri accelerometric recording (PGA 0.156g) of the Irpinia 1980, Ms 6.8 earthquake with a critical acceleration $K_c=0.045g$ equal to that used by Crespellani et al. (1996) for modeling the lower part of the Calitri landslide (slip surface 'A' in their analysis).

given by:

$$D=\int_0^t \int_0^t [a(t)-K_c g]\,\mathrm{d}t^2. \tag{9}$$

The double integration over time of the accelerations exceeding the critical acceleration gives the cumulative displacement; in the slope examined, the cumulative displacement is about 20 cm, in good agreement with that computed by Crespellani et al. (1996) for the slip surface 'A', corresponding to the lower part of the Calitri landslide.

In order to generalize the computed displacements as a function of the seismic parameters of the accelerometric recordings, theoretical slopes have been considered with critical acceleration normalized to PGA, that is:

$$K=\frac{K_c g}{\mathrm{PGA}}. \tag{10}$$

The parameter K is hereafter called the critical acceleration ratio. The critical acceleration ratio ranges between 0 and 1, and nine steps from 0.1 to 0.9 at an increment of 0.1 have been fixed, excluding the two extreme values. In fact, for $K=0$, the displacement goes to infinity, and for $K=1$, no coseismic displacements occur. Both K and K_c were used in the analyses that follow, as representatives of the resistance of the slope to failure.

4. Attenuation of landslide displacement

Displacements have been computed for each of the 95 couples of the horizontal components of acceleration time histories, selecting the component that provided the largest displacement.

The Italian seismic data set used for the regression analyses shown hereinafter relates the maximum computed displacement to PGA, I_A, and RMSA of each acceleration time history, according to the methodology pointed out by Jibson (1993), but using the critical acceleration ratio rather than critical acceleration.

In Fig. 4, the Newmark displacements versus Arias intensity are plotted for critical acceleration ratios between 0.1 and 0.8. The correlation coefficients range between 0.56 and 0.67, and all fits are significant above the 95% confidence level.

In Fig. 5, the best fits of computed displacements as a function of Arias intensity and RMSA for the nine steps of the critical acceleration ratios,

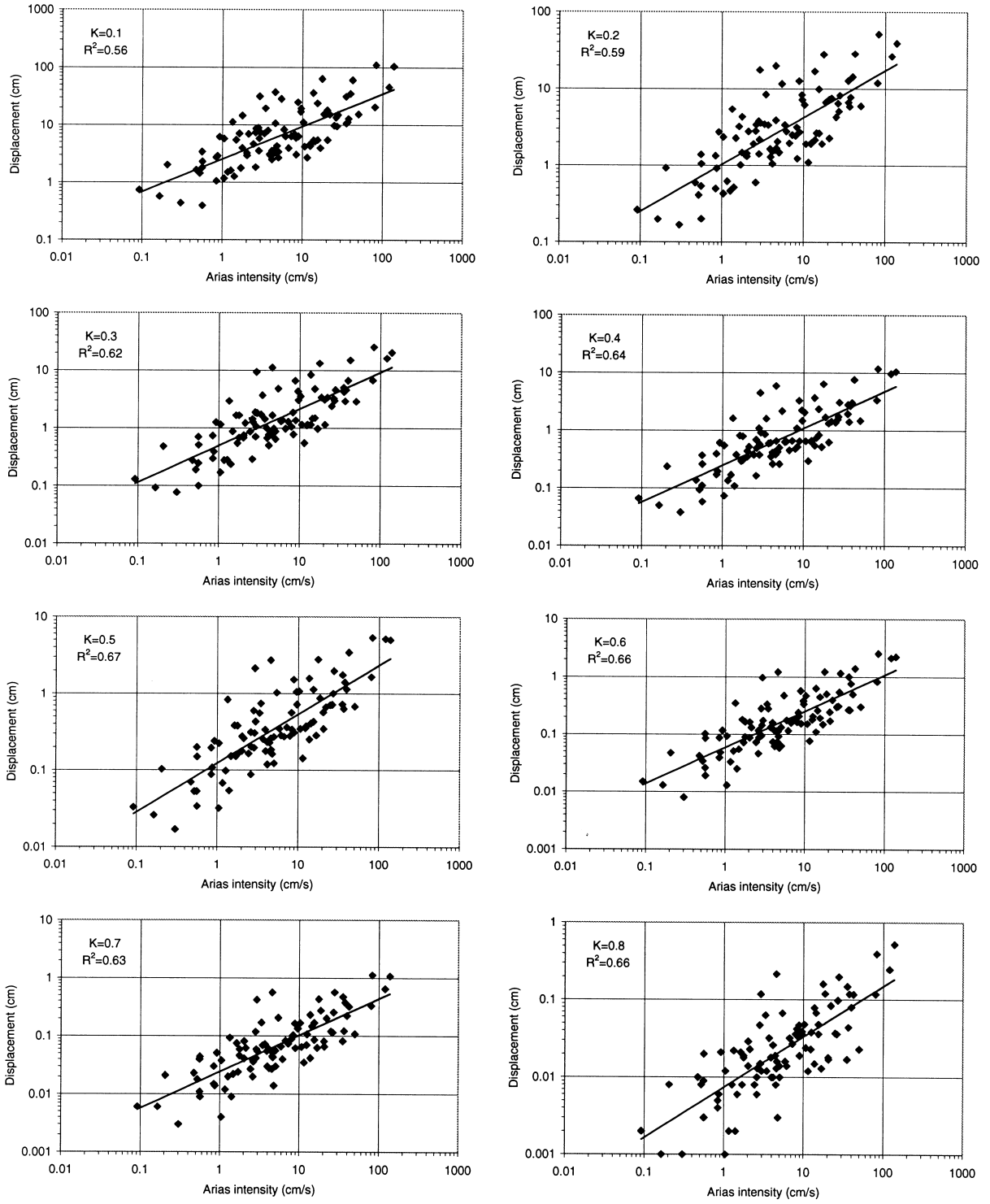

Fig. 4. Displacement versus Arias intensity for various critical acceleration ratios.

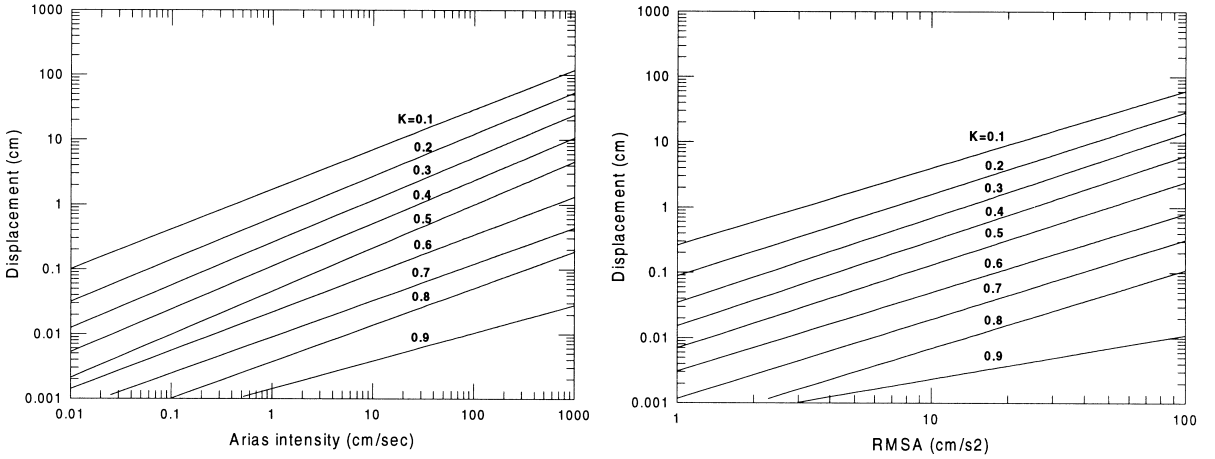

Fig. 5. Best fits of computed displacements for Arias intensity (left) and RMSA (right) for critical acceleration ratios between 0.1 and 0.9.

are shown. The lines fit almost parallel to each other and are equally spaced, suggesting a good multivariate correlation. The divergence from the parallelism for the critical acceleration ratio 0.9 shows a deviation from the linearity of the multiple correlation for critical accelerations very close to PGA; as K tends to 1, in fact, displacements tend to zero for any value of I_A or RMSA, so a tendency of the best-fit line to become parallel to the x-axis is to be expected as K approaches 1.

Multivariate regression analyses of the form:

$$\log_{10} D = f(\log_{10} I_A \quad \text{or} \quad \log_{10} \text{RMSA}, \quad K \quad \text{or} \quad K_c \quad \text{or} \quad \log_{10} K_c) \tag{11}$$

have been performed to search for the most significant correlation.

Table 1 synthesizes the results of the multivariate regression analyses; the statistical meaning of each regression is given by the adjusted squared multiple correlation coefficient (R^2) and the standard deviation of the logarithm of displacement ($\sigma_{\log D}$).

Table 1
Landslide displacements as a function of Arias intensity, RMSA and critical acceleration: results of the multivariate analyses

	K	K_c	Log K_c
Log I_A			
R^2	0.886	0.488	0.747
$\sigma_{\log D}$	0.365	0.799	0.562
Log RMSA			
R^2	0.864	0.490	0.761
$\sigma_{\log D}$	0.398	0.797	0.545

The correlation coefficient for RMSA is only slightly lower than for I_A when the parameter K is adopted to represent slope conditions; the same observation is reversed when K_c is used.

Although K_c is easier to use than K because it does not require knowing PGA, the most robust and statistically meaningful relation was obtained with the critical acceleration ratio, K (see Table 1). Thus, the best estimator of the coseismic displacements is a linear function of the critical acceleration ratio and a log-linear function of the Arias intensity:

$$\log_{10} D(\text{cm}) = 0.607(\pm 0.020) \log_{10} I_A (\text{cm/s}) - 3.719(\pm 0.049)K + 0.852(\pm 0.030) \pm 0.365. \tag{12}$$

For comparison, the same data set was analysed using the same variables as Jibson (1993). The results of the regression analyses are summarized hereinafter:

- a lower correlation coefficient (0.48 versus 0.87 from Jibson) is obtained when using critical acceleration instead of critical acceleration ratio, according to results shown in Table 1;

- the coefficient of log I_A is almost the same as in Jibson (1.414 versus 1.460), while the coefficient of the critical acceleration is higher (16.781 versus 6.642).

In conclusion, both Italian seismic data and the different form of the critical acceleration are responsible for the differences between the Jibson analysis and the present analysis.

Since the Arias intensity depends on the earthquake magnitude, the source-to-site distance, and the geologic site conditions, I_A has been expressed in terms of these variables:

$$I_A = f(M, R, S) \quad \text{then} \quad D = f(M, R, S, K). \tag{13}$$

According to Sabetta and Pugliese (1996), the best attenuation function of the landslide displacements fitting Italian strong-motion data is:

$$\log_{10} D = a + bM + c \log_{10} \times \sqrt{R^2 + d^2} + eK + fS + gR \pm \sigma \tag{14}$$

where M refers to local magnitude for $M \leq 5.5$ and to surface waves magnitude for $M > 5.5$, to ensure the best correlation as possible with moment magnitude (Hanks and Kanamori, 1979); R takes in turn the meaning of epicentral distance (RE) or the closest distance from the surface projection of the fault rupture (RF); and S has weight 0 for rock or stiff soils and 1 for soft soils (shear wave velocity not greater than 400 m/s and depth less than 20 m). The term S does not state that soil slopes can undergo greater displacements than rock slopes, since they only depend on the critical acceleration coefficient of the slope (depending, in turn, on shear strengths, geometric configuration and hydraulic conditions). Term S only accounts for the amplification of ground motion in soils compared to that which is observed in rock or stiff soils.

Coefficients a, b, c, e, f, and g are computed through a linear multivariate analysis, while coefficient d is calculated through a non-linear regression analysis and accounts for a fictitious focal depth. The term of anelastic attenuation, g, has been always found to be statistically meaningless and very close to zero. The results of the regression analyses are reported in Table 2.

The predictive models are expressed in terms of attenuation relations of the expected landslide displacements for both rock and soil slopes as a function of epicentral or fault distances:

$$\log_{10} D \quad (\text{cm}) = -1.144 + 0.591M - 0.852 \log_{10} \times \sqrt{\text{RF}^2 + 2.6^2} - 3.703K + 0.246S \pm 0.403 \tag{15}$$

$$\log_{10} D \quad (\text{cm}) = -1.281 + 0.648M - 0.934 \log_{10} \times \sqrt{\text{RE}^2 + 3.5^2} - 3.699K + 0.225S \pm 0.418. \tag{16}$$

The usefulness of such relations lies on the simple estimation of the expected magnitude and source–site distance for a reference earthquake (seismic scenario) to predict landslide displacements, as well as on the possibility to perform probabilistically based hazard analyses of expected landslide displacements.

Fig. 6 illustrates the results of a parametric analysis carried out to investigate the influence

Table 2
Attenuation of landslide displacements as a function of magnitude, distance, local site conditions and critical acceleration ratio: results of the multivariate regression analyses

Coefficients	Log D = $f(M$, log RF, K, $S)$	Log D = $f(M$, log RE, K, $S)$
a	-1.144 ± 0.125	-1.281 ± 0.134
b	0.591 ± 0.026	0.648 ± 0.030
c	-0.852 ± 0.041	-0.934 ± 0.051
d	2.6	3.5
e	-3.703 ± 0.055	-3.699 ± 0.057
f	0.246 ± 0.028	0.225 ± 0.029
g	0.0	0.0
R^2	0.861	0.851
$\sigma_{\log D}$	0.403	0.418

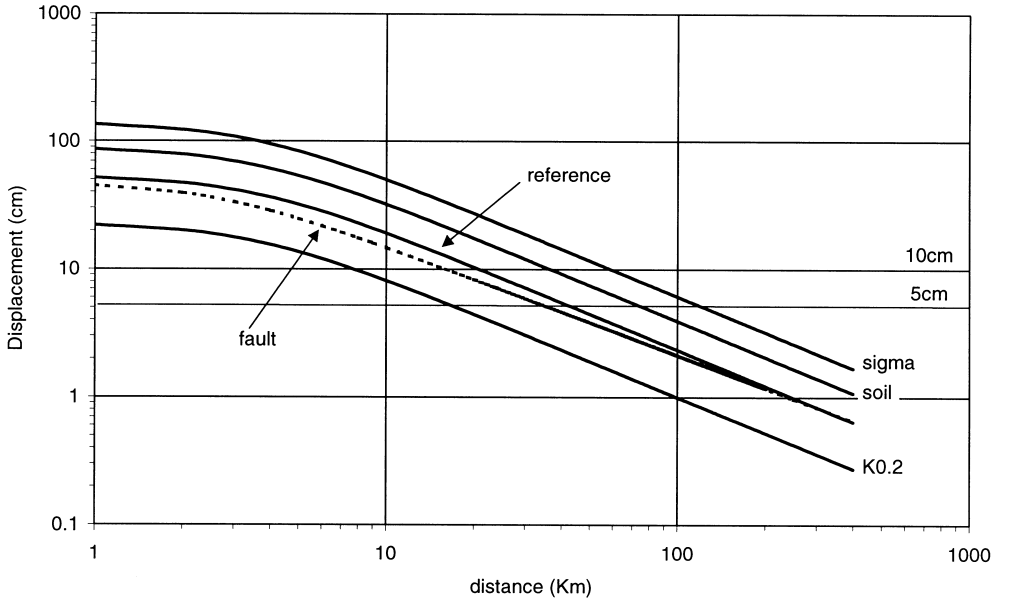

Fig. 6. Graphical illustration of the influence exerted by parameters of Eqs. (15) and (16) on the expected landslide displacements. The 'reference' curve has been drawn for an M6 earthquake, epicentral distances [Eq. (16)], a critical acceleration ratio of 0.1, a rock slope ($S=0$), and median values of computed displacements ($\sigma_{\log D}=0$). Curve 'fault' has the same parameters of the 'reference' but has been drawn using Eq. (15) (fault distance instead of epicentral distance). Curve 'sigma' has been plotted adding uncertainty in the computed displacements ($\sigma_{\log D}=1$). Curve 'soil' displays the attenuation of the landslide displacements for soil slopes ($S=1$) instead of rock slopes. Finally, the 'K0.2' curve has been drawn for a critical acceleration ratio twice the 'reference' one. Solid lines '10 cm' and '5 cm' show critical displacements for flows and disrupted slides, respectively.

exerted by the parameters of Eqs. (15) and (16). Comparisons are made with regard to a 'reference' curve whose parameters are: M6 earthquake, epicentral distances, critical acceleration ratio 0.1, rock slopes ($S=0$), and median values of computed displacements ($\sigma_{\log D}=0$).

Critical displacements (D_c) for disrupted and coherent slides (5 cm) and for flows or slides occurring in slopes that behave as viscoplastic materials (10 cm) are also shown in Fig. 6. Curve 'fault' refers to landslide displacements computed as a function of fault distance [Eq. (15)]. The same displacement is computed at a greater distance by Eq. (16) than by Eq. (15), by a definition of epicentral distance (a 20% of increment, on average), up to a distance of about 100 km. Nevertheless, fault distance attenuates less than epicentral distance, as its c-coefficient [the distance coefficient in Eq. (15)] shows.

Coefficient 'e' of the critical acceleration ratio is practically the same in both equations. When the uncertainty ($\sigma_{\log D}$) in the expected landslide displacements is considered, displacements that are a factor of 2.6 greater than the median displacements are predicted (curve 'sigma' in Fig. 6). The term 'S' exerts an influence that is about two-thirds of that exerted by $\sigma_{\log D}$, determining an increment of about 70% in the expected landslide displacements when taken into account. The same considerations can be argued for different reference earthquakes, that is for different magnitude values.

Eqs. (15) and (16) require the estimation of the expected PGA value. This can be easily done using published attenuation relations of the peak ground acceleration for Italy, such as those of Tento et al. (1992), Romeo et al. (1996), Sabetta and Pugliese (1996) and Rinaldis et al. (1998).

5. Discussion and applications

An immediate application of the methodology proposed in this work is the formulation of an

earthquake scenario in terms of expected landslide displacements. As an example, the spatial distribution of the expected landslide displacements reproducing the Irpinia 1980, Ms 6.8 earthquake is shown in Fig. 7A. The map is not slope-specific, that is the computed displacements [through Eq. (15)] are not referred to the actual critical accelerations of the slopes of the area; in fact, they have been calculated for virtual soil slopes with only one value of critical acceleration ratio ($K=0.1$). In the same figure, the largest landslides triggered by the Irpinia earthquake (D'Elia et al., 1985; Cotecchia, 1986) are shown together with the fault trace of the main rupture. Some landslides lie in the area where this simple model predicts displacements between 10 and 25 cm; for these landslides, triggered at a large distance from the fault rupture, a critical acceleration ratio close to 0.1 was plausible when the earthquake occurred.

Some real cases, among the landslides triggered by the Irpinia earthquake, have been examined to test the validity of the proposed methodology, and the results are summarized in Table 3, where, for each landslide (column A), the type of movement (B), the closest distance from the fault rupture (C) and the critical acceleration ratio (D), are reported. The landslide displacements, computed through the present methodology [Eq. (15), column G], are then compared with those (F) reported in specific studies (E). The results of the predicted displacements are in good agreement with the actual observations of the behavior of the landslides or with the dynamic analyses specifically carried out.

The Paola earth flow was reactivated 10 days after the main shock at a distance of 143 km from the closest point of the main fault rupture. Although intense rainfalls following the seismic event were the main causes of the reactivation, an important role was attributed to the earthquake in determining a shear strength reduction of the materials involved in the landslide (Cotecchia, 1986).

An alternative way to express the susceptibility of slopes to fail under seismic conditions is to perform a seismically induced landslide hazard analysis. Two methodologies and applications emerge from this study:

1. Derivation of the expected landslide displacements through relation (12). Fig. 7B shows the Arias intensity values expected to be exceeded at 10% probability level in 50 years (Romeo and Pugliese, 1998)[2]; it allows computation of the expected landslide displacements [through Eq. (12)] at the same probability level (namely, with an average return period of 475 years). Of course, landslide processes are not demonstrated to follow stationary models of occurrence as for earthquakes, so this map must be interpreted with care. It shows only that soil slopes in the darkest area with a critical acceleration ratio 0.1 or lower, for instance, could experience coseismic displacements equal to or greater than 57 cm, with a 10% chance of being exceeded in the next 50 years.
2. Derivation of the expected landslide displacements directly using relations (15) and (16). Fig. 7C and D shows two ways of expressing the potential landslide hazard assuming, as a merely illustrative example, that soil slopes may be characterized by a critical acceleration ratio of 0.1. Fig. 7C shows the annual probability exceeding the critical displacement of 10 cm, while in Fig. 7D, displacements that are expected to be exceeded at the 10% probability level in 50 years are depicted. Annual frequency probability maps, such as that in Fig. 7C, are useful to show the influence of frequent earthquakes on the expected landslide displacements; on the contrary, landslide hazard maps for long return period, such as that in Fig. 7D, highlight the influence of less frequent and higher energy seismic events. In the simplistic assumptions made for only illustrative purposes, Fig. 7B and 7D show that the maximum expected landslide displacements are similar using Eq. (12) (49–57 cm), and using Eq. (16) (50–60 cm). This convergence facilitates two alternative but similar ways to compute the expected displacements:
   1.1. estimate the PGA value for the proper magnitude–distance couple;

[2] Seismic hazard maps of Italy are available at the following web site: http://www.dstn.it/ssn/RT/rt9701/frameset.html.

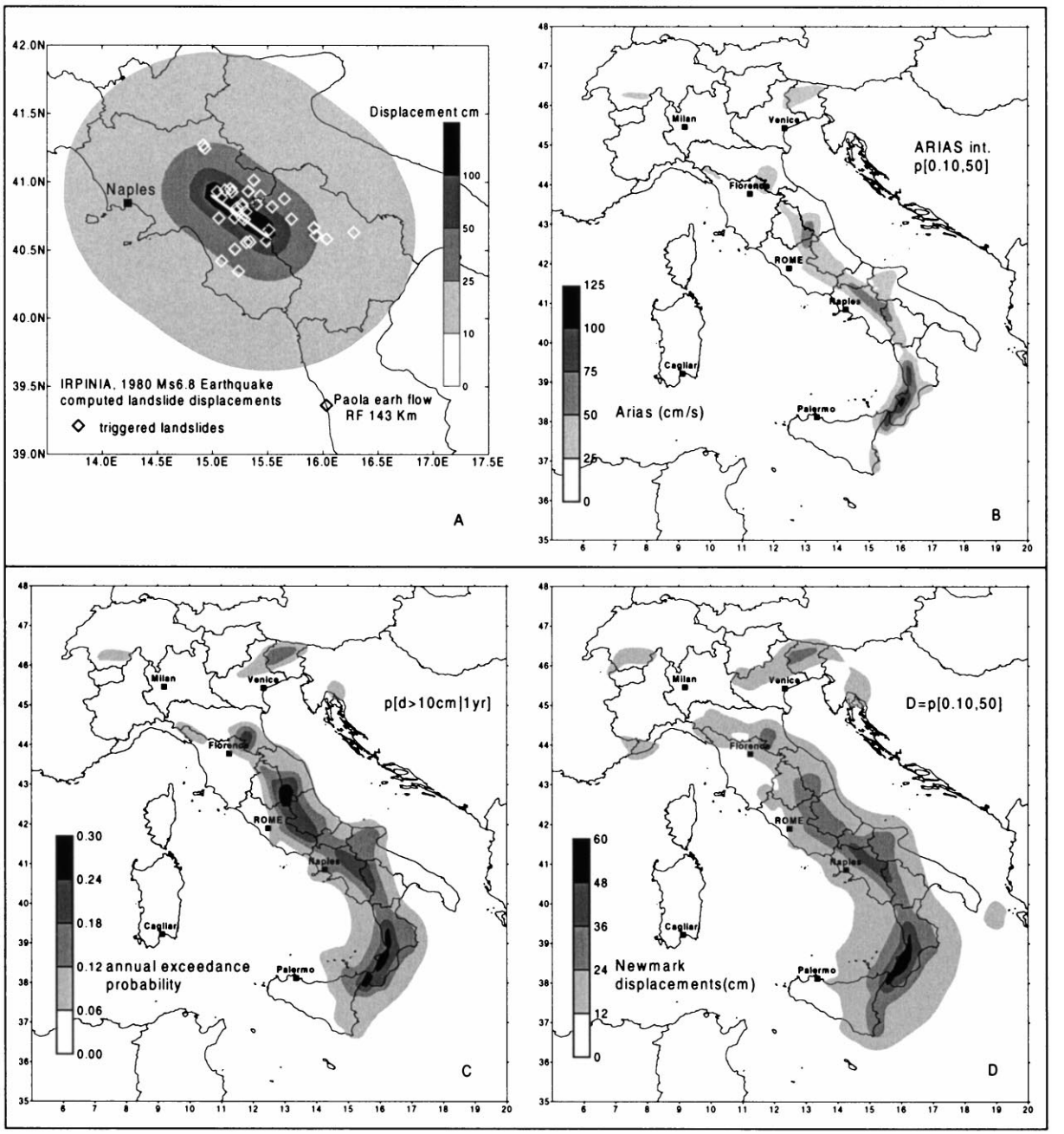

Fig. 7. (A) Example of spatial distribution of expected landslide displacements reproducing the Irpinia 1980, Ms 6.8 earthquake. Newmark displacements have been computed applying Eq. (15) and postulating, for only illustrative purposes, a critical acceleration ratio of 0.1. Open diamonds are location of the main landslides actually triggered by the earthquake. (B) Arias intensity expected to be exceeded at 10% probability level in 50 years (from Romeo and Pugliese, 1998, not shown). (C) Example of annual exceedance probability for 10 cm critical displacement of flows and slides occurring in highly plastic soils. (D) Example of calculation of the expected landslide displacements having a 10% chance of being exceeded in 50 years. These maps have been drawn referring, as a merely illustrative example, to virtual soil slopes having a critical acceleration ratio of 0.1 (see text).

Table 3
Comparison between displacements computed through the proposed methodology and displacements observed or calculated in site-specific studies for several landslides re-activated by the Irpinia 1980, Ms 6.8 earthquake

A. Locality where the landslide occurred	B. Kinematics of the landslide	C. Closest distance from the surface projection of the fault (km)	D. Critical acceleration ratio, K	E. Citation of the studies specifically carried out for each landslide	F. Observed or calculated* displacements (cm) reported in the site-specific studies cited in column E	G. Displacements (cm) computed through the present methodology applying Eq. (15)
Calitri	Rotational slide	20	0.07	Hutchinson and Del Prete, 1985; Crespellani et al., 1996	55*	56
Andretta	Rotational and translational slide	17	0.07–0.15	D'Elia, 1992	70–20*	65–33
Buonin-ventre	Mudslide	3	0.08	Cotecchia et al., 1986b; Del Prete and Trisorio Liuzzi, 1992	General collapse	174
Senerchia	Mudslide	9	0.06	Cotecchia et al., 1986a	General collapse	118
Pergola	Rotational slide	9	0.16	Cotecchia et al., 1986a	$\cong$30	50
S.Giorgio La Molara	Slide and earth flow	40	0.24	Dramis et al., 1982	Ground cracks	7

1.2. derive the expected I_A value from the relation given in Fig. 1;
1.3. compute the expected displacements through Eq. (12) at the specific K-value.
2.1. the same step as 1.1;
2.2. compute the expected displacements through Eq. (15) or Eq. (16) at the specific K-value.

For example, a soil slope with critical acceleration coefficient $K_c = 0.03g$ located 10 km from the epicenter of a M6 earthquake will experience a PGA value of about $0.3g$ (using Sabetta and Pugliese's, 1996 attenuation law), corresponding to an expected I_A of 52.97 cm/s (Fig. 1). The expected displacement at the critical acceleration coefficient $K = 0.1$ will be 33.6 cm from Eq. (12) applying methodology 1, versus 32 cm computed through Eq. (16) using methodology 2.

The concept that the maps in Fig. 7A–D represent neither an actual earthquake-induced landslide scenario nor a specific geographical distribution of the landslide hazard must be stressed. The maps need, in fact, to be combined with the actual geographical distribution of critical acceleration values and need to be represented at a detailed scale (regional or local).

6. Conclusions

A direct method to compute coseismic landslide displacements has been formulated. This couples the simplicity of evaluating earthquake triggering parameters with the susceptibility of slopes to undergo failure when subjected to cyclic loading.

Tests carried out on some real cases taken from landslides triggered by an M6.8 earthquake that occurred in southern Italy in 1980 (Irpinia earthquake) confirmed the validity of the proposed Eqs. (12), (15) and (16) for predicting seismically induced landslide displacements.

This method is also suitable for modeling earthquake-induced landslide scenarios and landslide hazard when maps of expected landslide displacements for various K-values (as in Fig. 7A, C and D) and maps showing the distribution of critical acceleration values are overlapped (Wieczorek et al., 1985; Luzi and Pergalani, 1996; Jibson et al., 1998; Miles and Hoxx, 1999).

I anticipate investigating other seismicity parameters such as the destructiveness potential (Uang and Bertero, 1988), which has been demonstrated to play a fundamental role in determining the structural response to strong shakings, as well as extending the concept of failure probability to landslide occurrence and recurrence probabilities to provide a forecasting where large landslide displacements are more likely to occur.

Acknowledgements

I wish to thank R. Jibson and D. Keefer (USGS), J. Wasowski (CNR/CE.RI.S.T.), and a fourth anonymous reviewer, for their helpful comments and criticism, which improved very much the paper. Special thanks to Prof. A. Prestininzi (University of Urbino), who continuously encouraged me to carry on this research.

References

Ambraseys, N.N., Menu, J.M., 1988. Earthquake-induced ground displacements. Earthquake Engineering and Structural Dynamics 16 (7), 985–1006.

Ambraseys, N.N., Srbulov, M., 1995. Earthquake induced displacements of slopes. Soil Dynamics and Earthquake Engineering 14, 59–71.

Arias, A., 1970. A measure of earthquake intensity. Seismic Design for Nuclear Power Plants. Massachussetts Institute of Technology Press, Cambridge, MA, pp. 438–483.

Bernard, P., Zollo, A., 1989. The Irpinia (Italy) earthquake: detailed analysis of a complex normal faulting. Journal of Geophysical Research 94 (2), 1631–1647.

Bishop, A.W., 1954. The use of pore pressure coefficient in practice. Geotechnique 4, 148–152.

Cotecchia, V., 1986. Ground deformations and slope instability produced by the earthquake of 23 November 1980 in Campania and Basilicata, Proceedings of the International Symposium on Engineering Geology Problems in Seismic Areas, IAEG, April 13–19, 1986, Bari, Italy Vol. 5., 31–100.

Cotecchia, V., Del Prete, M., Tafuni, N., 1986a. Effects of earthquake of 23rd November 1980 on pre-existing landslides in the Senerchia area (southern Italy), Proceedings of the International Symposium on Engineering Geology Problems in Seismic Areas, IAEG, April 13–19, 1986, Bari, Italy Vol. 4, 177–198.

Cotecchia, V., Lenti, V., Salvemini, A., Spilotro, G., 1986b. Reactivation of the large 'Buoninventre' slide by the Irpinia earthquake of 23 November 1980, Proceedings of the

International Symposium on Engineering Geology Problems in Seismic Areas, IAEG, April 13–19, 1986, Bari, Italy Vol. 4, 217–253.

Crespellani, T., Madiai, C., Maugeri, M., 1996. Analisi di stabilità di un pendio in condizioni sismiche e post-sismiche. Rivista Italiana di Geotecnica, XXX (1), 50–61.

D'Elia, B., Esu, F., Pellegrino, A., Pescatore, T.S., 1985. Some effects on natural slope stability induced by the 1980 Italian earthquake, Proceedings of the 11th ICSMFE, San Francisco, CA Vol. 4, 1943–1949.

D'Elia, B., 1992. Dynamic aspects of a landslide reactivated by the November 32, 1980 Irpinia earthquake (southern Italy), Proceedings of the French–Italian Conference on Slope Stability in Seismic Areas, May 14–15, 1992, Bordighera, Italy, 33–45.

Del Prete, M., Trisorio Liuzzi, G., 1992. Reactivation of mudslides after a long quiescent period the case of Buoninventre in southern Apennines, Proceedings of the French–Italian Conference on Slope Stability in Seismic Areas, May 14–15, 1992, Bordighera, Italy, 33–45.

Dramis, F., Prestininzi, A., Cognini, L., Genevois, R., Lombardi, S., 1982. Surface fractures connected with the southern Italy earthquake (November 1980) — distribution and geomorphological implications, Proceedings of the 4th International Congress of IAEG, December 10–15, 1982, New Delhi, India Vol. 8., 55–66.

Hanks, T.C., Kanamori, H., 1979. A moment magnitude scale. Journal of Geophysical Research 84, 2348–2350.

Housner, G.W., 1975. Measures of severity of earthquake ground shaking, Proceedings of the US National Conference on Earthquake Engineering, EERI, Ann Arbor, MI, June 1975, 25–33.

Hutchinson, J.N., Del Prete, M., 1985. Landslides at Calitri, southern Apennines, reactivated by the earthquake of 23rd November 1980. Geologia Applicata e ldrogeologia XX (1), 9–38.

Jibson, R.W., 1993. Predicting earthquake-induced landslide displacement using Newmark's sliding block analysis. Transportation Research Board, National Research Council, Washington D.C., TR record 1411, 9–17.

Jibson, R.W., Keefer, D.K., 1993. Analysis of the seismic origin of landslides examples from the New Madrid seismic zone. Geological Society of American Bulletin 105, 521–536.

Jibson, R.W., Harp, E.L., 1996. The Springdale, Utah, landslide: an extraordinary event. Environmental and Engineering Geoscience 2 (2), 137–150.

Jibson, R.W., Harp, E.L., Michael, J.A., 1998. A method for producing digital probabilistic seismic landslide hazard maps: an example from the Los Angeles, California, area. US Geological Survey Open-File Report 98-113. 17 pp., 2 pl

Keefer, D.K., 1984. Landslides caused by earthquakes. Geological Society of American Bulletin 95, 406–421.

Lambe, T.W., Whitman, R.V., 1979. Soil Mechanics. Wiley, New York. 553 pp.

Luzi, L., Pergalani, F., 1996. Applications of statistical and GIS techniques to slope instability zonation (1:50.000 Fabriano geologic map sheet). Soil Dynamics and Earthquake Engineering 15, 83–94.

Martin, P.P., Seed, H.B., 1978. APOLLO: a computer program for the analysis of pore pressure generation and dissipation in horizontal sand layers during cyclic or earthquake loading. Report No. UCB/EERC-78/21. Earthquake Engineering Research Center, University of California, Berkeley, CA.

Matsui, T., Ohara, H., Ito, T., 1980. Cyclic stress–strain history and shear characteristics of clay. Journal of Geotechnical Engineering Division, ASCE 106, GT10, 1101–1120.

Miles, S.B., Hoxx, C.L., 1999. Rigorous landslide hazard zonation using Newmark's method and stochastic ground motion simulation. Soil Dynamics and Earthquake Engineering 18, 305–323.

Newmark, N.M., 1965. Effects of earthquakes on dams and embankments. Geotechnique 15 (2), 139–159.

Rinaldis, D., Berardi, R., Theodulikis, N., Margaris, B., 1998. Empirical predictive models based on a joint Italian and Greek strong-motion database: I, peak ground acceleration and velocity. Proceedings of the 11th European Conference on Earthquake Engineering, September 6–11, 1997, CNIT, Paris La Defense, France.

Romeo, R., Tranfaglia, G., Castenetto, S., 1996. Engineering-developed relations derived from the strongest instrumentally-detected Italian earthquakes. Proceedings of the 11th WCEE, June 23–28, 1996, Acapulco, Mexico, Paper No. 1466.

Romeo, R., Delfino, L., 1997. Catalogo nazionale degli Effetti Deformativi del suolo Indotti da forti Terremoti. Rapporto Tecnico SSN/RT/97/04, Roma, Maggio 1997. 38 pp.

Romeo, R., Pugliese, A., 1998. A global earthquake hazard assessment of Italy. Proceedings of the 11th European Conference on Earthquake Engineering, September 6–11, 1997, CNIT, Paris La Defense, France.

Sabetta, F., Pugliese, A., 1996. Estimation of response spectra and simulation of nonstationary earthquake ground motion. Bulletin Seismological Society of America 86 (2), 337–352.

Sarma, S.K., 1981. Seismic displacement analysis of earth dams. Journal of Geotechnical Engineering Division, ASCE 107 (12), 1735–1739.

Tento, A., Franceschina, L., Marcellini, A., 1992. Expected ground motion evaluation for Italian sites, Proceedings of the 10th WCEE, July 19–24, Madrid, 489–494.

Uang, C., Bertero, V.V., 1988. Implications of recorded earthquake ground motions on seismic design of building structures. Report No. UCB/EERC 88/13. Earthquake Engineering Research Center, University of California, Berkeley, CA.

Vanmarke, E.H., Lai, S.P., 1980. Strong-motion duration and RMS amplitude of earthquake records. Bulletin Seismological Society of America 70, 1293–1307.

Wieczorek, G.F., Wilson, R.C., Harp, E.L., 1985. Map showing slope stability during earthquakes in San Mateo County, California. Miscellaneous Investigation Maps I-1257-E, U.S.G.S., 1985.

Wilson, R.C., Keefer, D.K., 1983. Dynamic analysis of a slope failure from the 6 August 1979 Coyote Lake, California, Earthquake. Bulletin Seismological Society of America 73 (3), 863–877.